Self-assembly of sp^2-bonded carbon nanostructures from amorphous precursors

R. C. Powles
School of Physics, A28, The University of Sydney, Sydney, New South Wales 2006, Australia

N. A. Marks
Nanochemistry Research Institute, Curtin University of Technology, P.O. Box U1987, Perth, Western Australia 6845, Australia

D. W. M. Lau
Applied Physics, School of Applied Sciences, RMIT University, GPO Box 2476V, Melbourne, Victoria 3001, Australia

(Received 25 September 2008; revised manuscript received 3 November 2008; published 18 February 2009)

Pure carbon phases such as fullerenes, nanotubes, and graphite are archetypal examples of the self-organizing capability of sp^2-bonded carbon. Naturally occurring phenomena and a wide variety of experimental apparatus are known to produce highly ordered sp^2-bonded carbons if the temperature or energy of the process is sufficiently high. Here we present molecular-dynamics simulations of sp^2 ordering using highly disordered amorphous carbon precursors. Using the environment-dependent interaction potential to describe the interatomic forces, we show that ordered sp^2 phases spontaneously arise upon heating at elevated temperatures. We identify two principal factors which control the collective organization: (i) the geometry of the system, in which clusters lead to onions, rods lead to nanotubes, and so on, and (ii) the effect of density, through which voids and internal surfaces control both local and long-range temporal evolutions. The simulations also shed light on the thermal stability of tetrahedral amorphous carbon and a fullerene-based structural model for glassy carbon.

DOI: 10.1103/PhysRevB.79.075430 PACS number(s): 61.43.Bn, 64.75.Yz, 61.46.Fg, 81.05.Tp

I. INTRODUCTION

Carbon is remarkable for the great structural variety of its pure solid forms, which can contain sp, sp^2, and sp^3 hybridized bonds, tending toward linear, planar, and tetrahedral geometries, respectively. Despite this flexibility, it is the predominantly sp^2-bonded structures which make up the greatest and most varied part of the carbon menagerie.[1] Highly ordered sp^2-bonded structures are found almost universally in nanoscale systems in which mobile carbon atoms have sufficient energy to rearrange. These structures, such as fullerenes, nanotubes, and graphite, have been observed as the products of many natural and synthetic processes characterized by high temperatures or large energy inputs. In addition to nanostructural forms, low-density bulk forms of carbon such as amorphous carbon (a-C), carbon foam,[2,3] activated carbon,[4] and glassy carbon[5] are also known to have high sp^2 fractions and varying degrees of local to medium-range order. Despite the ubiquity and technological significance of these highly ordered sp^2-bonded carbon materials, the processes which lead to their formation remain poorly understood. This is particularly the case for processes in which metal catalyst particles are absent.

There is an increasing body of experimental evidence which suggests that in the absence of a catalyst, fullerenes, nanotubes, and other sp^2-ordered carbons can be derived from the solid-phase transformation of amorphous carbon precursor or seed structures.[6,7] These solid-phase transformation processes are distinct from gas-phase nucleation processes which proceed through the agglomeration and rearrangement of molecular fragments.[8–10] Recent atomistic simulations which show fullerenes[3] and nanotubes[11] evolving from disordered and crystalline precursors under high-temperature conditions support this solid-phase "crystallization" [6,7] growth model. According to this model, amorphous carbon nanoparticles are formed early in the growth process with geometries related to the process conditions. As these particles are exposed to the high-temperature or high-energy-input conditions typical of laboratory or natural formation processes (plasma, combustion, or electron irradiation), a graphitization process is initiated at the particles' surface. This ordering process progresses from the surface toward the interior of the particles, eventually transforming them into concentric shells of sp^2-bonded atoms with a geometry (spherical or cylindrical) related to the shape of the original amorphous particles. We use the term "self-assembly" to describe this process since it produces highly ordered sp^2-bonded structures from disordered precursors, does not require a catalyst, and is thermodynamically driven.

The similarity in the cohesive energies of unstrained diamond and graphite bulk phases at room temperature is often noted. At the atomic scale, this translates to an energetic similarity between atoms with diamondlike sp^3-hybridized bonds and atoms with graphitelike sp^2-hybridized bonds. This raises a number of important questions about the formation process of highly ordered sp^2-bonded carbons: How can the observed self-assembly of ordered sp^2-bonded carbon structures be so efficient in the presence of such an energetic similarity between sp^2- and sp^3-bonding states? Why do such a wide variety of precursors (with varying microstructures and sp^2 fractions) convert readily into structures with a high sp^2 fraction? What is the role, if any, of sp^3-bonded atoms in the formation and final structure of high-sp^2-fraction materials? Is there an analog of the crystallization model which is relevant to the formation of *bulk* sp^2-rich carbons?

In this work, we address these questions by using molecular-dynamics (MD) simulations to explore the struc-

tural evolution of pure carbon systems under high-temperature annealing treatments. The MD simulations extend previous experimental observations in two significant ways, first by allowing direct access to the atomic-scale details and dynamics of the structural evolution process, and second by enabling the study of bulk materials without surface effects. Inspired by recent computational studies of carbon onions[3] and experimental studies of nanotubes,[7,12] we use highly disordered amorphous carbon as a precursor material. By varying the geometry and density of the precursor, we show the strong influence of the free surfaces on the subsequent evolution of highly ordered sp^2 structures. The influence of the annealing protocol on the development of extended sp^2 structures is also explored, which leads to observations which are relevant to the formation of bulk nongraphitizing and glassy carbons.

II. METHODS

MD simulations are performed using the environment-dependent interaction potential (EDIP).[13,14] EDIP gives an accurate description of bonding in amorphous and liquid carbon, and has recently been used to simulate thermal phenomena in carbon thin-film growth.[15,16] In crystalline phases, EDIP reproduces well the elastic constants of bulk diamond and sheets of graphite. Similarly, the method has high accuracy for long-range repulsive interactions present during the compression of graphite into diamond. For reasons of computational efficiency, the long-range interaction is truncated at 3.2 Å, and thus the van der Waals attraction between widely separated π-bonded sheets is absent. Due to the extremely high temperatures used in this work, the omission of these weak interactions has minimal effect. All calculations are performed in the *NVE* ensemble, enabling a systematic variation in the density. This is particularly useful for exploring low-density amorphous carbons which have received little attention. Other technical details follow common practice: temperature control is via velocity-scaling thermostats, numerical integration uses the Verlet method, and a time step on the order of 0.1 fs ensures energy conservation.

To create the sp^2-bonded networks, we first prepare amorphous carbon (*a*-C) precursor structures containing 4096 atoms and spanning densities between 1.5 and 3.0 g/cc. Synthesis of the *a*-C structures is achieved using the liquid-quenching method,[13] in which the amorphous state is generated by rapid quenching (0.5 ps) from an equilibrated liquid sample within a simple cubic supercell. It is well established that at system densities between 2.0 and 3.0 g/cc, these quenching conditions produce structures with sp^3 fractions and physical properties very similar to those of amorphous carbons produced experimentally by thin-film deposition.[14] In particular, this computational approach has had great success in describing tetrahedral amorphous carbon (*ta*-C).[17,18] Using these *a*-C structures as a common starting point, four sets of annealing simulations are performed to explore the effect of removing one or more of the periodic boundary conditions (PBCs). Where all three PBCs are removed the starting structure describes a cluster, where two are removed the structure is a wire or rod, and where one is removed the structure is a surface or film, while the retention of all three PBCs describes a bulk material. For convenience we denote these cases 0D (zero dimensional), 1D (one dimensional), 2D (two dimensional), and 3D (three dimensional), respectively. The annealing simulations are carried out at high temperatures (3000–4000 K) for extended periods (200 ps). As previously noted in our study of carbon onions (with 0D periodicity),[3] these annealing conditions produce highly evolved sp^2 networks which are structurally stable and do not change in any significant sense with further simulation time.

A. Network analysis

The simulated carbon systems are characterized using a variety of structural measures. Coordination fractions are measured by counting neighbors within a radius of 1.85 Å. In systems where one or more of the periodic boundary conditions are removed, clusters of atoms can become detached from the main cluster of atoms and drift outward in the simulation cell. We remove these atoms from the system before calculating the sp^2 fraction since they are not relevant to the rearrangement processes occurring in the main cluster. Shortest-path (SP) rings are identified using the algorithm of Franzblau.[19]

In order to characterize the medium- and long-range order in highly sp^2 networks, we compute the average normal vector of SP rings which contain only sp^2 atoms. The orientation of this vector with respect to an arbitrary fixed axis is defined, but its direction is not, so it is represented by a pair of angular coordinates related by reflection through the average plane of the ring. Plotting these coordinates gives a convenient, compact representation of the extent and type of sp^2 ordering in the simulated systems. We choose to plot the zenith and azimuthal angles projected onto Cartesian coordinates. The number of points on such a "normal vector orientation plot" is equal to twice the number of sp^2 rings in the system. The number of rings containing exclusively sp^2 atoms is an indicator of short-range ordering in a highly sp^2 system. Medium- and long-range ordering is reflected in the distribution of ring normal orientations. A tight clustering of points is caused by a group of highly correlated ring orientations which can only be due to sp^2 rings arranged in nearly planar sheets. A scattered distribution of points indicates that sp^2 rings are present but their orientations are not strongly correlated. This can occur when the rings form extended but highly curved sheets or many small randomly oriented sheet fragments.

B. Void volume calculations

In our analysis, a void is defined as a space where a probe particle can be inserted without overlapping the volume occupied by the atoms already in the system. The void volume is therefore determined by the exclusion radii of the atoms and the radius of the probe particle. To determine the total volume of void space in the simulated system, we use a method based on analyzing the Voronoi S-network of the atomic configuration.[20,21] Each site of the Voronoi S-network is the possible center of an interstitial sphere which touches

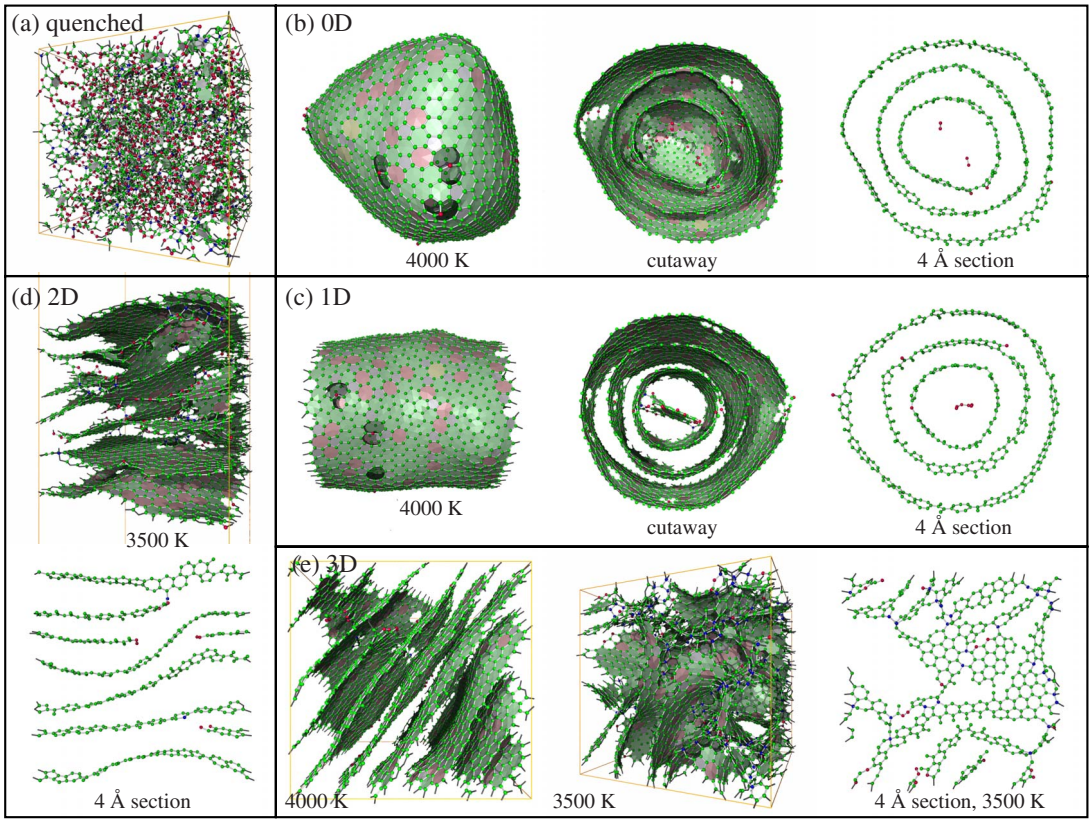

FIG. 1. (Color online) Simulations of a low-density (1.5 g/cc) amorphous carbon precursor system after 200 ps of high-temperature annealing which show the effect of the periodic boundary conditions of the simulation cell on the fully evolved structure. The development of extended sp^2 ordering is highlighted by rendering as surfaces all rings in which the atoms are exclusively sp^2 bonded. (a) 4096-atom amorphous carbon (*a*-C) precursor generated by liquid quenching at 1.5 g/cc. (b) (0D, isolated cluster) Final structure after annealing of the system in panel (a) at 4000 K for 200 ps with all three periodic boundary conditions removed. (c) (1D, nanowire) Same as (b) but with two periodic boundary conditions removed. (d) (2D, freestanding sheet) Same as (b) but with one periodic boundary condition removed and an annealing temperature of 3500 K. (e) (3D, bulk) Same as (b) but with all three periodic boundary conditions intact and annealing temperatures of 4000 K (left panel) and 3500 K (center and right panels). In the color version of this figure (online), some additional structural information not critical to the discussion is indicated: Atoms are colored by coordination: red (*sp*), green (sp^2), and blue (sp^3). Ring surfaces are colored by ring length: blue (5), green (6), red (7), and yellow (8).

adjacent atoms and encloses empty space. Interstitial spheres with radii larger than the probe radius are part of the void volume. Having established the center coordinates (Voronoi S-network sites) and radii of the interstitial spheres using the method of Medvedev,[21] we numerically estimate the total void volume by adding the contributions of all interstitial spheres with radii larger than the probe radius accounting for sphere overlap.

The exclusion radius of atoms in the system and the radius of the probe particle are variables in this type of analysis. We take the probe to be an additional carbon atom, so the probe and exclusion radii are equal and set to half the interaction cut-off distance for the pairwise terms in the EDIP potential.[13] This results in an exclusion radius of $r_{\mathrm{excl}}=1.3$ Å for a coordination of $Z=4$. We choose the $Z=4$ case since it is close to the upper limit of pairwise interaction lengths in our simulated systems. Other choices of the exclusion radius are possible, which will alter the total void volume. Void fractions over a similar range of densities for disordered carbon systems simulated using the AIREBO (adaptive intermolecular reactive empirical bond order) potential were presented by Stuart *et al.*[22] However these results were based on a definition of void space as all volume not occupied by atoms. This corresponds to using a probe particle of zero radius and leads to higher void fractions at all densities.

III. RESULTS

Figure 1(a) shows a 4096-atom 1.5 g/cc *a*-C system prepared using a liquid-quenching method. As would be anticipated given the low density (graphite has a somewhat higher density of 2.27 g/cc), the structure has high proportions of *sp* (36%) and sp^2 (58%) atoms, with sp^3 atoms present as only a minor species (6%). Extended high-temperature annealing of this disordered precursor using 0D, 1D, 2D, and 3D periodic boundary conditions produces profoundly different structures as shown in Figs. 1(b)–1(e). Although all of the annealed structures are predominantly sp^2 bonded and consist largely of extended sheets, the local sheet curvature and connectivity vary markedly. Despite these differences, the rate at which the system transforms into a nearly fully sp^2

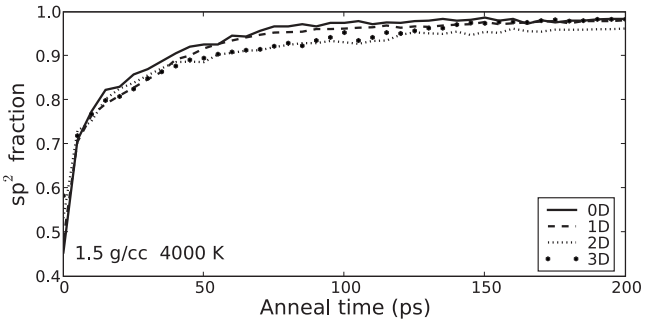

FIG. 2. Fraction of sp^2 atoms in the main cluster as a function of annealing time for 1.5 g/cc systems annealed at 4000 K under 0D, 1D, 2D, and 3D periodic boundary conditions.

structure is largely independent of the boundary conditions (Fig. 2). The saturation of the sp^2 fraction shows that the simulation anneal time is long enough to capture the time scale of the sp^2 conversion process.

A. Surface-initiated ordering

A striking feature of the 0D, 1D, and 2D PBC structures is that the geometry of the free surfaces of the precursor (corresponding to a cube in zero dimension, a square prism in one dimension, and a freestanding sheet in two dimensions) is reflected in the final annealed structures. In all these systems, the ordering process initiates at the external surfaces of the precursor. The surface atoms rapidly undergo almost complete conversion to sp^2 bonding and then rearrange into rings and ring clusters and finally into an extended sp^2 sheet which completely covers the surface. As the annealing progresses, there is a strong self-catalytic (or self-templated[23]) process which acts to convert the interior material adjacent to the surface sheet into a locally coplanar sp^2-bonded structure. In this way, the ordering progresses inward to convert the remainder of the enclosed material. This surface-driven ordering process determines the form of the annealed structure. Since it is energetically costly to break apart the extended sp^2 sheets once formed, the geometry of the surface sheet (which forms first) dictates the final geometry.

Figure 1(b) shows the 1.5 g/cc amorphous precursor after annealing at 4000 K for 200 ps after all periodic boundary conditions are removed (0D periodicity). The geometry of the precursor is an isolated cube of amorphous material with a side length of 38 Å. On annealing the system is converted into a concentric fullerene (or carbon "onion"). In previous work[3] we have shown that the appearance of onions on annealing is a robust process, in which the final structure is largely independent of the initial density and structure. In that study we found that amorphous networks at 1.5 and 2.0 g/cc (having high *sp* and sp^2 fractions) and 3.0 g/cc networks (dominated by sp^3 bonding) all produced onions on annealing. Similar behavior was observed using 3.5 g/cc nanodiamond precursors, although onions produced in this way exhibited slightly more radial ordering due to the higher symmetry of the precursor. As in the present study, ordering always proceeded from the outer surfaces (Fig. 3 of Ref. 3 shows intermediate stages of this process). Our simulations are supported by a variety of computational[24–26] and experimental studies[27,28] in which isolated nanoscale clusters of crystalline diamond have been observed to form carbon onions through surface-initiated ordering.

When two periodic boundary conditions are removed (corresponding to 1D periodicity), the precursor takes the form of a nanoscale rod. Upon annealing, this system is converted into a multiwall nanotube structure as seen in Fig. 1(c). We performed a variety of additional calculations (not reported here) in which the density and structure of the precursor were varied. As for the case of the onions in zero dimension, these had little effect on the final form of the annealed structure. Recent density-functional tight-binding simulations[11] also show surface-driven graphitization of nanodiamond rods and tubes. The crystallization model of nanotube growth was developed based on scanning electron microscopy (SEM) and transmission electron microscopy (TEM) observations of nanotube structures which appear to have been rapidly quenched or interrupted during growth.[6,7,29] These incompletely evolved tubes contain structural features consistent with the outside-in graphitization of an initially amorphous seed or precursor particle. Amorphous and graphitic seed particles are also observed in these samples. The conversion of amorphous carbon nanowires into multiwall nanotubes was recently observed in real-time experiments by Huang *et al.*[12] They applied resistive Joule heating to amorphous nanowires grown using a scanning tunneling microscope, and found that very high temperatures (above 2000 °C) produced nanotubes via a solid-state transformation. These extreme experimental temperatures are consistent with our work here where even higher temperatures are required to activate self-assembly on the subnanosecond time scale of the simulations. Very recently Du *et al.*[30] performed slightly different experiments which also illustrate this principle of self-assembly into nanotubes via annealing. Using wirelike nanostructures which were coalesced from glassy precursors, they observed nanotubes after annealing at 800–1000 °C. All of these results show that nanoscale carbon systems subjected to very high-temperature annealing (i.e., with sufficient kinetic energy) will self-assemble into highly ordered sp^2 structures.

When the system has two periodic boundaries, the precursor has a geometry corresponding to an infinite slab. Following the pattern that the symmetry of the annealed structure reflects the periodic boundary conditions, Fig. 1(d) shows that annealing produces ordered sp^2 sheets oriented parallel to the free surface. This results in a planar, layered configuration similar to crystalline graphite. As for both of the earlier cases, the conversion of sites to sp^2 bonding and the ordering into sheets are surface-initiated processes. Further examples of this behavior can be seen in our earlier EDIP simulations[31] of annealing in high-density (3.0 g/cc) amorphous carbon. The experimental equivalent of 2D periodicity is commonly found in carbon structures prepared as thin films. In the case of *ta*-C synthesized using ion-beam techniques, it has long been known that a monolayer or two of horizontally ordered graphitelike material exists at the film surface,[32] even though the interior of the material is amorphous and predominantly sp^3 bonded. The present work pro-

vides a helpful framework to understand such behavior. At the external surface the thin film relaxes toward a thermodynamic minimum consistent with the geometry, but high kinetic barriers prevent further graphitization of the interior of the film. This distinction between surface and bulk effects highlights the importance of the surface-to-volume ratio in all of the simulated systems discussed thus far. When the cluster size is very large, or the annealing temperature is not particularly high, the material at the center of the system will experience a more bulklike environment, and may in fact evolve in a different way if the cluster is sufficiently large. This point is elegantly illustrated in the amorphous nanowire experiments in which annealing of very thick nanowires produces horizontal nanotubelike ordering on the outside, but vertical graphitelike layers in the interior (Fig. 1 of Ref. 12). In contrast, only nanotubelike ordering is seen when the amorphous region is thin (Fig. 3 of Ref. 12).

B. Void-initiated ordering

The final case illustrated in Fig. 1 [panel (e)] is a system in which all three periodic boundary conditions are retained, which can be taken to represent bulk material with a density of 1.5 g/cc. In such systems external surfaces are by definition absent, and the high sp^2 fraction and extensive ordering cannot be due to the "outside-in" ordering process observed in nanoscale systems with free surfaces. Instead, we find in the bulk that sp^2 conversion and ordering is associated with internal voids. Just as the external surfaces of nanoscale precursors were rapidly converted into sp^2 sheet fragments, so too the internal surfaces of the voids rearrange into small graphitic domains. Depending on the size of the voids, these fragments may be highly curved. The ordering propagates from these void surfaces into the bulk material, creating further sp^2 sheet fragments. As noted above, this rearrangement mechanism can also be relevant in 0D, 1D, and 2D systems where the majority precursor material is not near an external surface. An important difference between the outside-in ordering of nanoscale precursors and the "inside-out" ordering initiated at voids is that in the latter case, sp^2 ordering is initiated at the surface of multiple voids simultaneously. Independent regions of sp^2 ordering can, either by themselves or by merging with adjacent regions, create structures which are topologically incompatible with the independent sheets of graphitic structures. Examples of such structures are closed shells, self-intersecting sheets, and Y junctions[33] where sp^2 sheets meet at high angle intersections and are linked by sp^3 atoms.

Typical microstructures associated with void-initiated ordering are illustrated in Fig. 1(e). Upon annealing the 1.5 g/cc system at 3500 K while retaining all periodic boundary conditions (3D), the system is transformed into a "foamlike" structure containing both planar and highly curved sp^2 sheets [Fig. 1(e), center panel]. This structure only contains 90% sp^2 bonding due to the sp^3 sites at junctions between sheets, and the sp sites which appear at sheet edges. When annealed at a higher temperature of 4000 K [left panel of Fig. 1(e)], the same precursor evolves to form a distinctly different graphitic microstructure in which the sp^2 sheets are largely planar. In this system the sp^2 fraction is 98%, reflecting the small number of defects such as sheet junctions involving sp^3 atoms. Normal vector orientation plots (Fig. 3) show the development of the medium- and long-range order under these two annealing conditions. After 200 ps of annealing the two systems are clearly very different. The scattered distribution of ring orientations shown in Fig. 3(a) corresponds to the 1.5 g/cc foamlike structure consisting of highly curved sheets as shown in the center panel of Fig. 1(e). The tightly clustered distribution of ring orientations shown in Fig. 3(b) corresponds to the 1.5 g/cc structure annealed at 4000 K which forms domains of "graphitelike" (coplanar flat sp^2 sheets) order as shown in the left panel of Fig. 1(e).

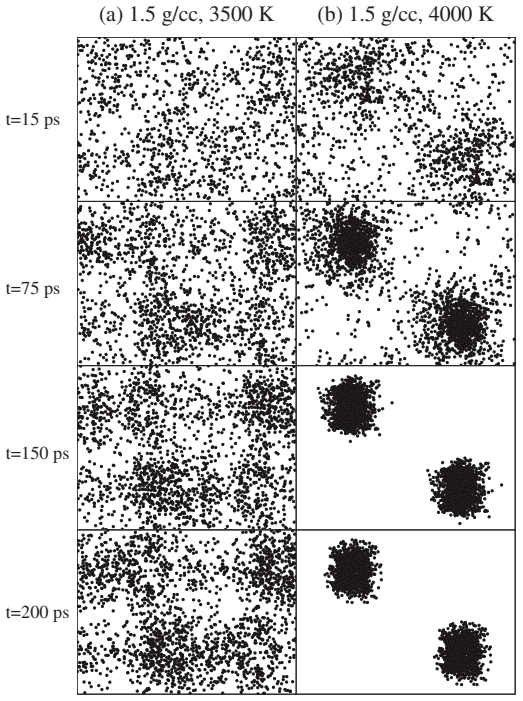

FIG. 3. Normal vector orientation plot (see Sec. II A) for sp^2 rings in a 1.5 g/cc 3D system annealed for 200 ps at (a) 3500 K [structure shown in Fig. 1(e), center and right panels], and (b) 4000 K [structure shown in Fig. 1(e), left panel].

To understand why the 3500 and 4000 K systems evolve so differently, we consider the atomic processes required to rearrange the amorphous precursor. The development of medium- and long-range order evident in Figs. 1 and 3 requires substantial atomic rearrangement and the energy barriers associated with this process can be overcome more easily at higher annealing temperatures. Long-range graphitic order develops in the 1.5 g/cc system annealed at 4000 K, as the entire system is able to rearrange in order to reach the global minimum potential-energy configuration. At the lower annealing temperature of 3500 K, there are some energy barriers to rearrangement which cannot be overcome during the simulation time. In this case, the system cannot rearrange arbitrarily, and instead local and medium-range sp^2 order develops near voids where the energy barriers to rearrangement are lowest. The sp^2 structures which are the result of this process (curved sheets, Y junctions, etc.) are themselves very stable structures (low potential energy) when compared to

amorphous atomic arrangements. The energy penalties for rearranging the low-temperature annealed foamlike system into graphite are in fact larger than for the amorphous system. In effect, the system annealed at 3500 K has become trapped in a deep valley of the configurational energy landscape.[34,35] Further evolution of this system toward graphitization occurs on a much slower time scale compared to the initial local and medium-range sp^2-ordering processes. This is due to the large barriers which must be overcome to "undo" locally ordered stable structures which are topologically incompatible with the long-range graphitic order.

We thus see that the thermal history (annealing protocol) strongly influences the structural evolution of the system. The important insight from this work is that the annealing protocol does not simply determine the extent of system evolution along a common pathway from the amorphous initial state toward graphite. The development of local and medium-range sp^2 order in low-density systems at lower annealing temperatures leads to a distinct family of high-sp^2-fraction foamlike structural forms which evolve much more slowly toward graphitization than the initial amorphous material.

To support this interpretation, we subjected the system already annealed at 3500 K for 200 ps to a further 200 ps of annealing at 4000 K. The sp^2 fraction increased from 90% to 95%, and the sp^3 fraction reduced from 6% to 2%. Furthermore, the sp^2 sheets were able to reorganize into a single graphitic domain, albeit one with curved sheets and some topological defects. Visually, the structure is intermediate between the two 1.5 g/cc structures shown in Fig. 1(e). Given the appearance of the single domain, we strongly suspect that further annealing will eliminate the remaining defects and lead to complete graphitization. Compared to the reorganization which occurred during the first anneal at 3500 K, the changes which occur on the second anneal proceed much more slowly, and the final structure is still less ordered than the system annealed at 4000 K for 200 ps from the as-quenched amorphous state.

To quantify the role of voids in these bulk systems, we computed the void fraction of liquid (5000 K) and quenched (300 K) systems at a number of densities. Figure 4 shows that the void fraction in both liquid and quenched systems is nonzero below 2.5 g/cc, and at the lowest density considered (1.5 g/cc), the void fraction is very significant, accounting for around one-third of the total volume. Due to the very rapid quench rates, the amorphous structures are closely related to the liquids from which they are derived. We note also that the void fraction at 1.5 g/cc behaves as would be intuitively expected, with liquid carbon, amorphous carbon, and annealed carbon having progressively higher void fractions due to the increasing local order.

In addition to confirming the presence of voids at low densities, Fig. 4 provides a useful physical view of rearrangement processes in disordered carbon. According to our definition of void space (see Sec. II B), where the void fraction is nonzero, the system contains voids large enough to accommodate additional unbonded atoms. Voids of this dimension are particularly relevant to diffusion and rearrangement processes. In materials with strong directional bonding such as carbon, there are large energy barriers for atomic

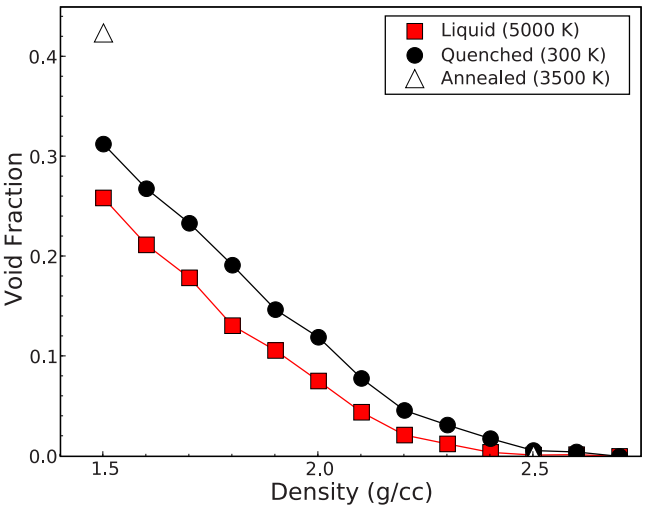

FIG. 4. (Color online) Void fraction as a function of density for systems simulated under 3D periodic boundary conditions at a temperature of 5000 K and after rapid quenching to 300 K. At densities below 2.5 g/cc, the simulated systems have a nonzero void volume. Also shown are the void fractions for 1.5 and 2.5 g/cc systems annealed for 200 ps at 3500 K (open symbols). At 1.5 g/cc, the void fraction increases on annealing, while at 2.5 g/cc the void fraction remains close to zero. A probe and exclusion radius of $r_{\mathrm{excl}} = 1.3$ Å are used to calculate the void volume (see text).

motions which require the displacement of surrounding atoms. When void spaces are available which allow atoms to move beyond the range of attractive interaction forces, diffusion and rearrangement may occur at a significantly higher rate. Figure 4 thus provides an intuitive explanation for the rapid sp^2-ordering behavior observed at 1.5 g/cc.

Due to the nonzero void fraction in bulk precursors with densities lower than 2.5 g/cc, we may expect void-initiated ordering to be significant for other amorphous carbons across this density range. We also explored 2.0 g/cc amorphous precursors (annealed at 3500 and 4000 K for 200 ps), and observed foamlike and layered structures similar to those shown in Fig. 1. However, at densities approaching and exceeding 2.5 g/cc, we can expect very different behavior since the void-initiated sp^2-ordering mode is not available and thus different types of structures will evolve upon annealing. Such materials are considered in Sec. III C.

C. Void-free bulk amorphous precursors

We now consider the evolution of amorphous carbon precursors with densities such that the void volume is close to zero ($\gtrsim 2.5$ g/cc). For nanoscale amorphous precursors, the primary role of the precursor density is to alter the rate at which the structure evolves toward a highly ordered sp^2 form. Although the initial density of the precursor determines whether or not internal voids are present in the system, all nanoscale precursors have free external surfaces. Free external surfaces permit surface-initiated ordering processes and systemwide density changes to occur. On high-temperature annealing, all nanoscale amorphous carbon precursors with large surface area–to–volume ratios are observed to trans-

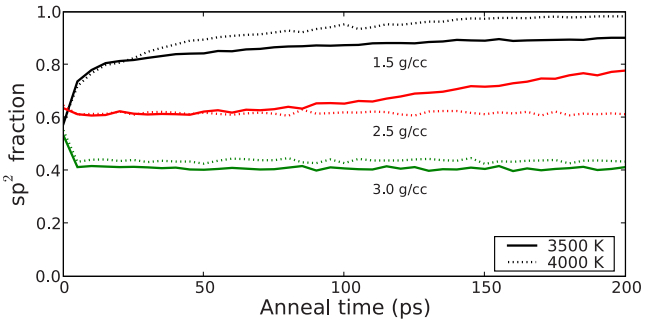

FIG. 5. (Color online) Fraction of sp^2 atoms in the main cluster as a function of annealing time for 1.5, 2.5, and 3.0 g/cc systems annealed at 3500 K (solid line) and 4000 K (dashed line) under 3D periodic boundary conditions.

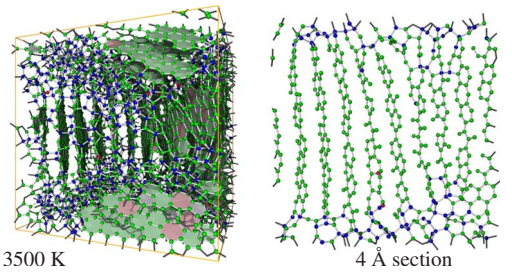

FIG. 6. (Color online) Simulation of a 2.5 g/cc amorphous carbon precursor system after 200 ps of annealing at 3500 K with 3D periodic boundary conditions on the simulation cell. The cross section in the right-hand panel shows the layered structure within some of the graphitelike domains. Legend for color version of this figure (online) is same as for Fig. 1.

form into highly ordered sp^2 structures via these routes (see Sec. III A). The final structure has little dependence on either the initial density or atomic arrangement of the precursor. In the remainder of this section we consider the annealing behavior for bulk systems and/or regions far from external surfaces.

Figure 5 shows the sp^2 fraction with anneal time for 1.5, 2.5, and 3.0 g/cc systems annealed at 3500 and 4000 K under 3D PBCs. The sp^2 fraction increases rapidly at the beginning of the anneal for 1.5 g/cc systems, and as discussed above, initially amorphous regions of mixed coordination are converted into highly ordered sp^2-rich domains. For the 2.5 g/cc system annealed at 3500 K, an increase in sp^2 fraction is also observed, but at a much slower rate. In contrast, the sp^2 fraction is constant throughout most of the anneal for 2.5 g/cc systems annealed at 4000 K, despite the high temperature and long annealing time. At 3.0 g/cc, the sp^2 fraction decreases sharply and the structure becomes predominantly sp^3 bonded. After less than 10 ps of annealing the structure is stable, and no ordering of sp^2 atoms occurs.

There are two possible explanations for the lack of sp^2 ordering at higher densities. First, sp^2 bonding might not be the lowest-energy configuration, and hence there is no driving force for the system to evolve in that direction. Another possibility is that sp^2 ordering is still favorable, but the time scale for ordering has changed by many orders of magnitude. The slow evolution of the 2.5 g/cc system at 3500 K illustrates the second of these effects. Here we can see that the system is gradually evolving toward a predominantly sp^2 network, but the time scale of the rearrangement is much slower than at 1.5 g/cc. We only observe rapid ordering when surfaces (external and voids) are present, but at 2.5 g/cc this ordering mechanism is heavily suppressed because the void fraction is low. Indeed, the surprising observation that 4000 K annealing at 2.5 g/cc inhibits sp^2 formation suggests this system is close to a threshold separating sp^2 and sp^3 regions. Our interpretation of this result is that the high temperature is pressurizing the fixed-density system, thereby inhibiting the transformation to a purely sp^2-bonded phase.[36]

Figure 6 shows the final state of a 2.5 g/cc system after 200 ps of annealing at 3500 K. Multiple graphitelike domains of ordered sp^2-bonded sheets are present, connected by extended regions of sp^3-rich amorphous material. The coexistence of distinct structures strengthens our hypothesis that this density is close to a boundary above which the sp^3 phase is dominant. The ordering within the sp^2 regions of Fig. 6 demonstrates another density-driven effect, namely, that in the absence of voids curved sp^2 sheets cannot form. As a consequence, graphitic ordering will be more likely to evolve at intermediate densities as compared to lower densities since topological defect structures (which generally require curved sheets and, thus, voids) are no longer accessible in the early stages of annealing.

Figure 7(a) shows the time evolution of the 2.5 g/cc structure in Fig. 6. The system contains three graphitic domains as shown by the six clusters of points on the normal vector orientation plot (recall that each point appears twice on the plot). The nucleation of these domains (seen in the figure as

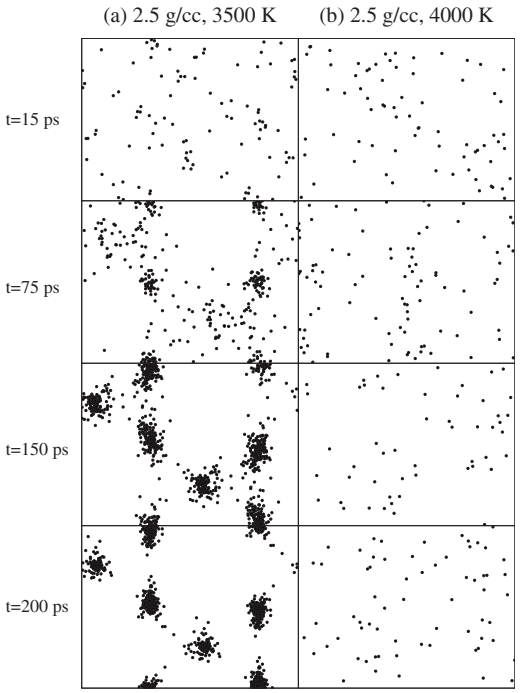

FIG. 7. Normal vector orientation plot for sp^2 rings in a 2.5 g/cc system annealed at (a) 3500 and (b) 4000 K, under 3D periodic boundary conditions for 200 ps. The construction of this plot is the same as in Fig. 3.

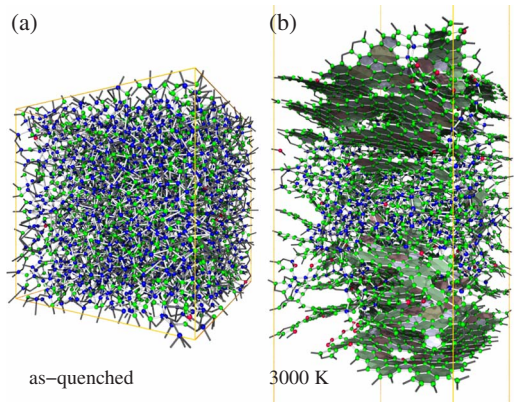

FIG. 8. (Color online) Simulations of a 3.0 g/cc amorphous carbon precursor system: (a) as-quenched structure and (b) after 200 ps of annealing at 3000 K with 2D periodic boundary conditions on the simulation cell [same scale as (a)]. Legend for color version of this figure (online) is same as for Fig. 1.

highly correlated sp^2 ring orientations) is a slow process, requiring ~100 ps before the domains become fully distinct. Since this process is slow, the domains develop independently, leading to small grains as seen in Fig. 6. The development of order at 2.5 g/cc contrasts markedly with the other system in which we observe graphitic ordering (1.5 g/cc annealed at 4000 K). In the lower-density system (where large voids are present), order appears rapidly over an extended region, with the nucleation center becoming apparent after just 15 ps [Fig. 3(b)].

Figure 7(b) shows that at an annealing temperature of 4000 K, the 2.5 g/cc system does not develop extended regions of sp^2 ordering. While there are isolated rings consisting of sp^2 atoms, clustering of rings does not occur, and the number of rings does not increase in number with time. Visual inspection of the structure (not shown) confirms the absence of any extended sp^2 ordering and shows that the entire structure is amorphous. This is perhaps surprising given that the sp^2 fraction remains close to 60% throughout the anneal (Fig. 5). As noted earlier, our interpretation is that sp^2 ordering is suppressed by pressurization associated with the higher temperature.

At the highest density considered in Fig. 5 (3.0 g/cc), the system is predominantly sp^3 bonded. Amorphous carbon synthesized at this density by rapid quenching produces realistic tetrahedral amorphous carbon (*ta*-C) structures. On annealing with 3D periodic boundaries at both 3500 and 4000 K, the simulated *ta*-C network is extremely stable, despite the very high temperatures and long annealing times. Visual inspection of the initial and final structures shows both to be dense amorphous networks which are virtually indistinguishable. However, when the system is annealed with 2D periodic boundaries, the upper and lower surfaces are able to relax. Figure 8 shows both the as-quenched structure at 3.0 g/cc and the system after 200 ps of annealing at 3000 K with 2D periodic boundaries. In this example the outside-in ordering discussed earlier is clearly apparent. The bulklike region at the center has not changed (consistent with the 3D annealing result), while the outer layers experience a progressive graphitization and a corresponding decrease in density. The expansion of the system is primarily driven by the structural transformation rather than pressure in the precursor system. This is confirmed by observing that early in the annealing time, before significant structural transformations occur near the surfaces, the change in system size is modest. Any pressure-driven expansion would be expected to occur very rapidly after the 2D boundary conditions were imposed. The surface graphitization observed in this 2D system is a more dramatic demonstration of an effect noted in passing in earlier EDIP simulations.[31] The important contribution of the present work regarding *ta*-C annealing is the combination of the 2D and 3D annealing simulations. We see from the 3D calculations that even with extremely high temperatures and (comparatively) long annealing times, the bulk material under fixed-density conditions remains stable and the sp^3 fraction remains high. It is only when free surfaces are available that the surface layers are able to transform, allowing a progressive layer-by-layer transformation which will eventually consume the bulklike interior. Viewing this process from an experimental perspective yields an important insight; namely, that experiments measuring the thermal stability of bulk *ta*-C are in fact probing the thermal stability of the *outer layers*. We thus have the intriguing possibility that the thermal stability of bulk *ta*-C could in fact be higher than the typical values of 1000 and 1400 K as determined by Anders *et al.*[37] and Ferrari *et al.*,[38] respectively. One might, for example, coat the surface of the *ta*-C film with a high-melting-point material, inhibiting the surface relaxation and thereby increasing the thermal stability of the sp^3 phase.

IV. NONGRAPHITIZING AND GLASSY CARBONS

Glassy carbon is a technologically significant material most commonly produced by the pyrolysis of suitable resin or polymer precursors at high temperatures under an inert atmosphere.[39,40] The resulting material typically has a density between 1.4 and 1.9 g/cc and is particularly valued for its chemical inertness and extreme thermal stability (resisting graphitization at temperatures of up to 3000 °C).[5] While the atomic-scale structure of glassy carbon is not fully established, it is known that the sp^2 fraction is very high, the local (≈5 Å) structure is highly ordered, but at longer length scales the structure is translationally and orientationally disordered (turbostratic). Various hypothetical schemes for the medium- and long-range structure and connectivity of the ordered sp^2 regions have been proposed.[40–43] These schemes attempt to reconcile the proposed structure with observations of electrical conductivity, gas infiltration, and chemical reactivity as well as structural probes such as TEM and x-ray diffraction.

Harris and Tsang[43,44] suggested that glassy carbon may consist of "fullerene-related structures" (i.e., sp^2 sheets containing five-, six-, and seven-membered rings) based on high-resolution TEM observations of sp^2 sheets with high curvature including closed shells. Their proposed structure consists of broken and imperfect fullerene fragments which can be multilayered and which often surround open pores or voids. This structure is more compatible with the observed permeability and reactivity of glassy carbons than competing

models which are based on tangled "ribbons" of sp^2 sheets.[40,42] Recently, direct evidence for the presence of five-membered rings in low-density activated carbon materials has been obtained using aberration-corrected TEM imaging,[4] which supports the idea that fullerene-related structures may be present and thermally stable in related materials. An algorithm for generating an atomic structure based on the model of Harris[44] for the purpose of studying gas permeation was described by Terzyk *et al.*[45] This method is based on the stochastic assembly of specific fullerene fragments, and not on a physical process. Kumar *et al.*[46] used Monte Carlo simulation to evolve the structure of a low-density amorphous carbon precursor (based on the backbone of a polymer structure folded into a simulation cell with 3D PBCs) and reported that the resulting structure consists of a disordered arrangement of curved sp^2 sheets. While their structures [see Fig. 2(c) of Ref. 46] bear some resemblance to our low-density simulated structures generated using molecular dynamics, in the Monte Carlo algorithm only sp^2 bonding is allowed. This restriction prevents the formation of sp^3-bonded structural elements such as the sheet junctions and other topological defects which appear to play an important role in the thermal stability of our simulated systems. In our simulations, these topological defects only require a small sp^3 fraction ($\approx 5\%$), and their presence in nongraphitizing carbons would be very difficult to detect. A molecular-dynamics study of heat-treated low-density amorphous carbons with relevance to the synthesis of porous carbon materials was conducted by Shi.[47] In this work a new interatomic potential for carbon was developed in which sp^3 bonding was prohibited. As with the studies of Kumar *et al.*,[46] the evolved structures in the study of Shi[47] consist of curved sp^2 sheets, and have some visual resemblance to this study. However, the absence of sp^3 connectivity produces networks which are necessarily topologically distinct from those in this work, where the possibility of sp^3 is permitted.

The MD simulations in this work show that thermally stable structures consisting of a disordered arrangement of highly curved sp^2 sheets can be generated via a physically plausible (but not necessarily practical) route. It is significant that physically motivated "bottom-up" approaches (this work and those of Shi[47] and Kumar *et al.*[46]) generate structures which are very similar to the entirely hypothetical networks proposed by Harris and Tsang.[43] Figure 9 shows the remarkable similarity between a 19 Å cut through the 1.5 g/cc structure annealed at 3500 K [shown in Fig. 1(e), center panel] and an illustration of the hypothetical structure consisting only of fullerene-related fragments. Although definitive experimental evidence for the atomic structure of glassy carbon is still lacking, the convergence of hypothetical and bottom-up approaches is encouraging support for the validity of this model.

An important result of the MD simulations concerns the mechanism by which fullerene fragments can be generated. As we have shown, the presence of voids in the low-density amorphous carbon precursor provides a route to the formation of closed shells and highly curved sp^2 sheet fragments via the surface-initiated ordering process. Furthermore, our simulations show that systems containing these structural elements are stable at high annealing temperatures. We relate this to the high-energy barriers for the rearrangement of local structures which are topologically incompatible with the separate sp^2 sheets of graphite.

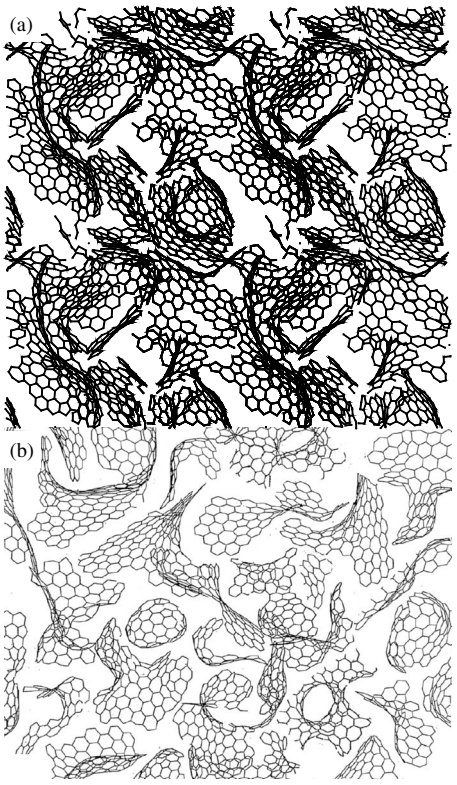

FIG. 9. The highly curved sp^2 sheet structure we observe in annealed low-density systems is very similar to a hypothetical structure for glassy carbon proposed by Harris (Ref. 44). (a) A 19 Å section of the 1.5 g/cc system annealed at 3500 K for 200 ps under 3D periodic boundary conditions. Several periodic images are included to highlight the medium- and long-range structure. Only bonds are shown, where bonds are drawn between atoms closer than 1.85 Å. Bonds crossing the boundaries of the section are not drawn. (b) Hypothetical fullerene-related structure proposed for glassy carbon by Harris (Ref. 44). From P. J. F. Harris, "Fullerene-related structure of commercial glassy carbons," Philos. Mag. 84, 3159 (2004). Copyright 2004. Reprinted by permission of Taylor & Francis Group (http://www.informaworld.com).

These topological defect structures appear to naturally arise in the presence of voids in the precursor due to the simultaneous growth and subsequent interaction of ordered sp^2 regions surrounding each void on annealing at moderate temperatures. This suggests a possible physical interpretation of the tendency of various precursor materials to graphitize or form nongraphitizing structures. We have shown that the size and distribution of internal voids in the precursor material (or formed during pyrolysis) as well as the annealing protocol can have an important influence on the structural evolution of the system. If local and medium-range sp^2 ordering dominates early in the thermal evolution, stable defect structures can be formed which dramatically increase the resistance of the material to further graphitization. Presumably, these structural rearrangement mechanisms would operate simultaneously with the complex array of other physicochemical processes which occur during pyrolysis. As discussed

earlier, the annealing protocol can influence not only the rate of evolution of the structure, but also the structural form itself. Annealing at different temperatures can lead to two families of structures: those which completely graphitize and thermally stable foamlike structures which graphitize far more slowly. This helps to explain why the properties of experimentally prepared glassy carbon depend so strongly on the preparation conditions and the precursor material.

V. CONCLUSIONS

Using molecular dynamics as a tool to evolve carbon networks, we have shown that fully disordered carbon structures subjected to high-temperature annealing spontaneously self-assemble to form highly ordered sp^2-bonded networks. We find that carbon onions arise from amorphous clusters, that carbon nanotubes emerge from amorphous nanowires, and that graphite sheets appear from amorphous slabs. Each of these results is independent of the initial configuration, confirming that even the most disordered carbon precursor can evolve toward order if sufficient kinetic energy is provided. The simulations provide a framework for understanding the evolution of carbon networks, and are supported in a number of specific instances by various experimental and computational studies. The nature of the final structure is heavily influenced by the presence of free surfaces, be they external surfaces determined by geometry at the nanoscale, or internal surfaces associated with voids. In systems with no external surfaces we highlight the important role of the void fraction, and show that above densities of 2.5 g/cc the collective rearrangement into sp^2-dominated forms is prohibited. The latter result has implications for understanding experimental annealing studies of tetrahedral amorphous carbon (*ta*-C). The simulations reveal that thermal transformation into sp^2-bonded forms is a surface-initiated process. Hence the thermal stability of bulk *ta*-C might in fact be higher than previously thought. In low-density bulk carbon we find a close connection between our evolved networks and hypothetical models of glassy carbon consisting of fullerenelike elements. Unlike previous works, we show that sp^3 sites are an important component of the microstructure of annealed bulk carbons, providing linkage elements required to accommodate grain boundaries, sheet junctions, and regions of high curvature. Finally, we show that the thermal history of annealed bulk carbons influences not only the rate of structural evolution, but also the structural form itself.

ACKNOWLEDGMENTS

Helpful discussions with David McKenzie and Dougal McCulloch are gratefully acknowledged.

[1] J. L. Delgado, M. A. Herranz, and N. Martin, J. Mater. Chem. **18**, 1417 (2008).
[2] K. Umemoto, S. Saito, S. Berber, and D. Tomanek, Phys. Rev. B **64**, 193409 (2001).
[3] D. W. M. Lau, D. G. McCulloch, N. A. Marks, N. R. Madsen, and A. V. Rode, Phys. Rev. B **75**, 233408 (2007).
[4] P. J. F. Harris, Z. Liu, and K. Suenaga, J. Phys.: Condens. Matter **20**, 362201 (2008).
[5] P. J. F. Harris, Crit. Rev. Solid State Mater. Sci. **30**, 235 (2005).
[6] P. J. F. Harris, Carbon **45**, 229 (2007).
[7] D. Zhou and L. Chow, J. Appl. Phys. **93**, 9972 (2003).
[8] Y. Yamaguchi, L. Colombo, P. Piseri, L. Ravagnan, and P. Milani, Phys. Rev. B **76**, 134119 (2007).
[9] N. Pineau, L. Soulard, J. H. Los, and A. Fasolino, J. Chem. Phys. **129**, 024708 (2008).
[10] S. Irle, G. S. Zheng, Z. Wang, and K. Morokuma, J. Phys. Chem. B **110**, 14531 (2006).
[11] V. V. Ivanovskaya and A. L. Ivanovskii, Inorg. Mater. **43**, 349 (2007).
[12] J. Y. Huang, S. Chen, Z. F. Ren, G. Chen, and M. S. Dresselhaus, Nano Lett. **6**, 1699 (2006).
[13] N. Marks, J. Phys.: Condens. Matter **14**, 2901 (2002).
[14] N. A. Marks, N. C. Cooper, D. R. McKenzie, D. G. McCulloch, P. Bath, and S. P. Russo, Phys. Rev. B **65**, 075411 (2002).
[15] N. A. Marks, Diamond Relat. Mater. **14**, 1223 (2005).
[16] N. A. Marks, M. F. Cover, and C. Kocer, Appl. Phys. Lett. **89**, 131924 (2006).
[17] N. A. Marks, D. R. McKenzie, B. A. Pailthorpe, M. Bernasconi, and M. Parrinello, Phys. Rev. Lett. **76**, 768 (1996).
[18] D. G. McCulloch, D. R. McKenzie, and C. M. Goringe, Phys. Rev. B **61**, 2349 (2000).
[19] D. S. Franzblau, Phys. Rev. B **44**, 4925 (1991).
[20] M. G. Alinchenko, A. V. Anikeenko, N. N. Medvedev, V. P. Voloshin, M. Mezei, and P. Jedlovszky, J. Phys. Chem. B **108**, 19056 (2004).
[21] N. N. Medvedev, V. P. Voloshin, V. A. Luchnikov, and M. L. Gavrilova, J. Comput. Chem. **27**, 1676 (2006).
[22] S. J. Stuart, M. T. Knippenberg, O. Kum, and P. S. Krstic, Phys. Scr. **T124**, 58 (2006).
[23] J. Y. Huang, F. Ding, K. Jiao, and B. I. Yakobson, Small **3**, 1735 (2007).
[24] G. D. Lee, C. Z. Wang, J. J. Yu, E. Yoon, and K. M. Ho, Phys. Rev. Lett. **91**, 265701 (2003).
[25] A. Brodka, T. W. Zerda, and A. Burian, Diamond Relat. Mater. **15**, 1818 (2006).
[26] J. M. Leyssale and G. L. Vignoles, Chem. Phys. Lett. **454**, 299 (2008).
[27] Z. J. Qiao, J. J. Li, N. Q. Zhao, C. S. Shi, and P. Nash, Scr. Mater. **54**, 225 (2006).
[28] S. Tomita, A. Burian, J. C. Dore, D. LeBolloch, M. Fujii, and S. Hayashi, Carbon **40**, 1469 (2002).
[29] P. J. F. Harris, S. C. Tsang, J. B. Claridge, and M. L. H. Green, J. Chem. Soc., Faraday Trans. **90**, 2799 (1994).
[30] G. X. Du, C. Song, J. H. Zhao, S. Feng, and Z. P. Zhu, Carbon **46**, 92 (2008).
[31] N. A. Marks, M. F. Cover, and C. Kocer, Mol. Simul. **32**, 1271 (2006).
[32] C. A. Davis, G. A. J. Amaratunga, and K. M. Knowles, Phys.

Rev. Lett. **80**, 3280 (1998).
[33] T. Kawai, S. Okada, Y. Miyamoto, and A. Oshiyama, Phys. Rev. B **72**, 035428 (2005).
[34] D. J. Wales, *Energy Landscapes* (Cambridge University Press, Cambridge, UK, 2003).
[35] D. J. Wales and T. V. Bogdan, J. Phys. Chem. B **110**, 20765 (2006).
[36] A. Y. Belov and H. U. Jager, Diamond Relat. Mater. **14**, 1014 (2005).
[37] S. Anders, J. Diaz, J. W. Ager, R. Y. Lo, and D. B. Bogy, Appl. Phys. Lett. **71**, 3367 (1997).
[38] A. C. Ferrari, B. Kleinsorge, N. A. Morrison, A. Hart, V. Stolojan, and J. Robertson, J. Appl. Phys. **85**, 7191 (1999).
[39] J. W. Lawson and D. Srivastava, Phys. Rev. B **77**, 144209 (2008).
[40] G. M. Jenkins and K. Kawamura, *Polymeric Carbons* (Cambridge University Press, Cambridge, 1976).
[41] I. Alexandrou, H. J. Scheibe, C. J. Kiely, A. J. Papworth, G. A. J. Amaratunga, and B. Schultrich, Phys. Rev. B **60**, 10903 (1999).
[42] L. A. Pesin and E. M. Baitinger, Carbon **40**, 295 (2002).
[43] P. J. F. Harris and S. C. Tsang, Philos. Mag. A **76**, 667 (1997).
[44] P. J. F. Harris, Philos. Mag. **84**, 3159 (2004).
[45] A. P. Terzyk, S. Furmaniak, P. A. Gauden, P. J. F. Harris, J. Wloch, and P. Kowalczyk, J. Phys.: Condens. Matter **19**, 406208 (2007).
[46] A. Kumar, R. F. Lobo, and N. J. Wagner, Carbon **43**, 3099 (2005).
[47] Y. F. Shi, J. Chem. Phys. **128**, 234707 (2008).